

Linking the Gut Microbiome to Neurocognitive Development in Bangladesh Malnourished Infants

Theo Portlock^{1,*}, Talat Sharma^{2,*}, Shahria Hafiz Kakon^{2,*}, Berit Hartjen^{3,*}, Chris Pook^{1,*}, Brooke Wilson^{1,*}, Ayisha Bhutto³, Daniel Ho¹, Inoli Shennon Wadumesthrige Don¹, Anne-Michelle Engelstad³, Renata Di Lorenzo³, Garrett Greaves³, Caroline Kelsey³, Peter Gluckman¹, Justin O'Sullivan^{1,4,5,6}, Terrence Forrester⁷, and Charles Nelson³

¹The Liggins Institute, University of Auckland, NZ

²Infectious Diseases Division, International Centre for Diarrheal Disease Research,
Bangladesh

³Department of Pediatrics, Boston Children's Hospital and Harvard Medical
School; Harvard Graduate School of Education, Boston, USA

⁴The Maurice Wilkins Centre, The University of Auckland, New Zealand

⁵MRC Lifecourse Epidemiology Unit, University of Southampton, University
Road, Southampton, UK

⁶Singapore Institute for Clinical Sciences, Agency for Science Technology and
Research, Singapore

⁷Faculty of Medical Sciences, UWI Solutions for Developing Countries, The
University of the West Indies (UWI), Jamaica

*These authors contributed equally

21 Glossary

22 **FDR** False Discovery Rate.

23 **HC** Head Circumference.

24 **LMIC** low- and middle- income countries.

25 **MAM** Moderate Acute Malnutrition.

26 **MUAC** Mid-upper arm circumference.

27 **MWU** Mann-Whitney U test.

28 **P/B** *Prevotella*-to-*Bacteroides*.

29 **PCoA** Principal Coordinates Analysis.

30 **PERMANOVA** permutational multivariate analysis of variance.

31 **SCFA** Short Chain Fatty Acid.

32 **SHAP** SHapley Additive exPlanations.

33 **WLZ/WHZ** weight-for-length/height.

34 Key points:

- 35 • The gut microbiome of malnourished infants is compositionally distinct from well-nourished
36 infants, characterised by a lower shannon diversity, higher *Prevotella*-to-*Bacteroides* ratio,
37 and lower potential anaerobic pathways involved in the fermentation of pyruvate.
- 38 • Depletion of plasma lipids critical for brain development were negatively correlated with gut
39 microbiome pathways, EEG power spectral density, and cognitive outcomes.
- 40 • There was a high level of commonality in the shared features between malnutrition and low
41 expressive communication.

42 Abstract

43 Malnutrition, affecting approximately 30 million infants annually, has profound immediate and
44 enduring repercussions, with nearly half of child deaths under 5 linked to malnutrition. Survivors
45 face lasting consequences, including impaired neurocognitive development, leading to cognitive
46 and behavioural deficits, impacting academic performance and socioeconomic outcomes. Despite
47 extensive literature on malnutrition’s mechanisms spanning nutrition, infection, metabolism, mi-
48 crobiome, and genomics, knowledge gaps persist. This study employs AI random forest models to
49 identify non-overlapping connections between the gut microbiome, plasma lipids, and EEG data,
50 from infants with Moderate Acute Malnutrition (MAM) and well-nourished controls. Plasma lipids
51 are significant contributors to the prediction of the MAMs condition. *Bacteroides fragilis* abun-
52 dance, linked to fermentation pathways, emerges as a predictive factor for well-nourished infants.
53 In conclusion, network analysis highlights the potential significance of targeted interventions in
54 addressing both the short and long-term impacts of malnutrition.

55 Key words

56 Malnutrition, Gut microbiome, Neurocognitive development, Plasma lipidome, Random Forest
57 classification models

58 Background

59 Malnutrition is a significant global health issue responsible for an estimated 45% of all child
60 deaths worldwide, making it the leading cause of mortality among children under the age of five¹.
61 Malnutrition is characterised by delayed growth, proportionate reductions in mass of most organs
62 and tissues, and alterations in tissue architecture². Children who survive malnutrition are likely
63 to suffer long-term consequences including impaired neurocognitive development, leading to long-
64 term deficits in cognition and behaviour³. This consequently leads to poor school performance
65 and economic prospects as an adult⁴. While much is known about the health, social, and economic
66 ramifications of malnutrition, significant gaps in our knowledge remain. One crucial gap is the

67 contribution of the gut microbiome to the pathology of malnutrition in addition to its impact on
68 brain and cognitive development.

69 The human gut microbiome is a complex ecosystem comprised of the microorganisms lining the
70 intestinal tract, including bacteria, viruses, fungi, and archaea. Infancy represents a sensitive
71 period in gut microbiome formation as the gut microbiome changes drastically over this time⁵.
72 Importantly, many aspects of malnutrition including host nutritional status, dietary intake, an-
73 tibiotic administration, and infections impact the diversity, composition, and functionality of the
74 microbiome^{6;7}. To this end, several studies in low- and middle- income countries low- and middle-
75 income countries (LMIC) have shown differences in gut microbiome profiles between malnour-
76 ished and well-nourished infants^{8;9}. For example, a study in Bangladesh found that malnourished
77 infants, compared to well-nourished infants, had higher abundances of *Bifidobacterium* and *Es-*
78 *cherichia* species¹⁰. Beyond the correlational and descriptive evidence presented, work using mouse
79 models point to a possible causal role of the gut microbiome in growth and weight gain, as mice
80 colonized using fecal microbial transplantation with samples from malnourished children, but not
81 well-nourished controls, showed impairments in weight gain and growth¹¹. Critically, perturba-
82 tions of the gut microbiome associated with malnourishment may have downstream consequences
83 for brain and cognitive development^{12;13}.

84 Malnutrition, like the gut microbiome, is associated with neurocognitive impairments thought to
85 result from structural and functional changes to the brain^{14;15;16;17;18;19}. More specifically, several
86 studies conducted in healthy infants living in upper-middle-income countries have shown that the
87 gut microbiome is associated with cognitive and brain development; although the directionality
88 remains unclear with both increased and decreased gut microbiota alpha diversity being linked
89 to positive cognitive outcomes and neural development^{13;15;20;21}. Previous research has suggested
90 that malnutrition may be associated with alterations in the gut microbiome, including changes
91 in the composition and diversity of the microbial community²². Moreover, alterations in the gut
92 microbiome may contribute to negative neurological outcomes observed in malnourished infants,
93 potentially through the disruption of nutrient absorption or the generation of toxic metabolites²³.
94 Very few studies have examined the link between the gut microbiome and cognition in malnour-
95 ished children. One notable exception is a randomized control trial of nutrition, stimulation, and
96 hygiene education in a group of rural Ugandan mothers and their infants who were moderately
97 stunted (HAZ scores between -2 and -3 SD). Across a series of studies conducted from 2 years to

98 3 years of age there were mixed findings with some species such as *Bifidobacterium longum* found
99 to associate with language impairment assessed using the Bayley Scales of Infant and Toddler
100 Development and other developmental assessments but at other time points no associations were
101 found^{17;24;25}. Therefore, more work is needed to understand how the gut microbiome mediates
102 that association between malnourishment and cognitive development.

103 Another mechanism by which brain and behavioural development may be impacted by malnutri-
104 tion is through the circulating plasma lipidome^{26;27}. Several circulating plasma lipids including
105 cholesterol, phosphatidylcholines, phosphatidylethanolamine, and sphingolipids compromise 50%
106 of the dry weight of the brain and have unique roles in neurological structure and function²⁸.
107 The brain relies upon nutrients circulating in the blood for its supply of resources. Moreover,
108 the blood brain barrier which plays a crucial role in regulating which circulating lipids enter and
109 exit the brain area is impaired by malnutrition²⁹. Circulating plasma lipids represent a means of
110 communication between the gut microbiome and the brain³⁰ and therefore represent a potential
111 mechanism of influence.

112 Given the importance of the composition and functions of the gut microbiome in maintaining
113 overall health, there has been increasing interest in understanding how its alterations may con-
114 tribute to malnutrition and its associated impacts on infant neurocognitive development. The
115 present study examines the impact of malnutrition on the composition of the infant gut micro-
116 biome, plasma lipidome, neural activity, and cognitive outcomes in a cross-sectional cohort of
117 well-nourished and malnourished 12-month-old Bangladeshi infants. Random forest models were
118 used to integrate deeply phenotyped multi-modal data and identify correlations that provide pu-
119 tative mechanistic insights into developmental delays the result from malnutrition. Overall, this
120 study provides important information about gut-blood-brain-behaviour links in infants impacted
121 by malnutrition.

Results

Study population characteristics

As a city with the second highest density of population and in a country with childhood malnutrition rate is one of the highest globally, the Mirpur region in Dhaka, Bangladesh was chosen to assess the impact of early-life malnutrition³¹. 156 infants with Moderate Acute Malnutrition (MAM) and 74 well-nourished controls at 12 months of age were recruited from this region (Figure 1a). MAM was defined according to WHO guidelines, using a threshold between two and three standard deviations below the mean z-score for weight-for-length/height (WLZ/WHZ)³². Confounding variables to measures of MAM (WLZ/WHZ, Mid-upper arm circumference (MUAC), Weight, and Head Circumference (HC)) were measured using Fisher's exact test for categorical variables and Mann-Whitney U test (MWU) for continuous variables. Significant confounding variables were the principal toilet used (Septic-tank/toilet), water treatment method (Boil), toilet facility (shared with other households), how long they lived in current household, mother's income, years of father education, father's education level, monthly total expenditure, and mother's occupation (housewife).

Malnutrition is associated with a higher *Prevotella-to-Bacteroides* (P/B) ratio and lower pyruvate fermentation potential in the gut of Bangladeshi infants

It was hypothesised that malnutrition impacts the diversity and composition of the infant gut microbiome in this cohort. Stool metagenomes were extracted, analysed (shotgun metagenomic sequencing, 40.53 ± 8.5 million reads with no significant difference between MAM and well-nourished (MWU $p=0.71$)) and profiled according to their species and functional compositions. Across all samples, we detected 3 kingdom, 17 phylum, 31 class, 51 order, 100 family, 226 genus, 749 species, 611 Functional Pathways, and 2,828,874 Gene Families.

There was a mean species richness of 50.3 ± 16.4 per sample, commensurate with other infants at that age group. Malnutrition was associated with a lower Shannon diversity (MWU $p=0.025$) and Pielou's evenness (MWU $p=0.009$) than their well-nourished counterparts (Fig-

Table 1: Baseline infant characteristics. Plus minus values are means \pm SD and their pvalues are calculated using MWU. All other values are categorical and their pvalues are calculated using Fishers Exact test.

	Malnourished (n=156)	Well-nourished (n=73)	pval
Principal toilet used: Septic-tank/toilet	103 (66.0%)	66 (90.4%)	0.000
Water treatment method: Boil	70 (44.9%)	50 (68.5%)	0.000
WLZ.WHZ (z-score)	-2.24 \pm 0.26	-0.22 \pm 0.48	0.000
MUAC (cm)	12.4 \pm 0.49	14.27 \pm 0.6	0.000
Weight (kg)	6.81 \pm 0.53	8.59 \pm 0.69	0.000
HC (cm)	43.01 \pm 1.32	43.93 \pm 1.35	0.000
Other expenses	1743.59 \pm 2154.34	2928.77 \pm 3554.01	0.001
Toilet facility shared with other households	128 (82.1%)	48 (65.8%)	0.010
How long lived in current household (years)	5.44 \pm 6.33	3.86 \pm 5.28	0.012
Mothers income	1395.51 \pm 3073.98	616.44 \pm 2072.51	0.022
Years of Father Education	5.01 \pm 3.67	6.41 \pm 4.29	0.031
Fathers education level	4.93 \pm 3.5	6.19 \pm 3.83	0.031
Monthly Total expenditure (taka)	14820.83 \pm 6409.76	18495.89 \pm 10919.18	0.037
Mothers occupation: Housewife	115 (73.7%)	63 (86.3%)	0.040
Household head's income	14378.21 \pm 6418.82	18958.9 \pm 18216.63	0.064
Place of Cooking: Outdoors	99 (63.5%)	37 (50.7%)	0.080
Days after birth	355.6 \pm 17.33	359.55 \pm 15.96	0.095
Family expenditure	10060.9 \pm 4790.9	12164.38 \pm 7675.29	0.115
Birth order of enrolled child among live births	1.78 \pm 0.99	1.58 \pm 0.82	0.150
Female	74 (47.4%)	28 (38.4%)	0.200
Household members using mobile phone	2.06 \pm 0.98	2.3 \pm 1.19	0.254
Drain	77 (49.4%)	42 (57.5%)	0.260
Household: Own house	46 (29.5%)	27 (37.0%)	0.290
Before eating: Soap	95 (60.9%)	50 (68.5%)	0.300
Nuclear family	90 (57.7%)	48 (65.8%)	0.310
Total monthly Income (taka)	19537.18 \pm 8697.86	25253.42 \pm 21158.65	0.338
Number of siblings under 5 years	0.56 \pm 0.84	0.56 \pm 0.62	0.358
Mother education level	5.53 \pm 3.26	6.18 \pm 3.68	0.359
Years of Mother Education	5.58 \pm 3.38	6.42 \pm 4.19	0.359
Before feeding child: Soap	75 (48.1%)	40 (54.8%)	0.400
Number of people sleeping in household	4.9 \pm 1.71	4.78 \pm 1.67	0.436
Number of members in your household	4.9 \pm 1.71	4.78 \pm 1.67	0.436
Number of living children	1.86 \pm 1.01	1.88 \pm 0.87	0.553
Number of rooms in current household	1.53 \pm 0.81	1.59 \pm 0.85	0.566
Other member's income	3011.54 \pm 5693.41	4945.21 \pm 9937.15	0.874
Other sources income	751.92 \pm 3206.54	732.88 \pm 2645.86	0.879

ure 1, ??). These differences in diveristy were underscored by a significant difference in the Bray-Curtis dissimilarity (permutational multivariate analysis of variance (PERMANOVA), $R^2=2.22$, $p=0.008$), as a consequence of the differential abundance of 6/350 species (1.7%) (Figure 1b, ??). There was a greater prevalence and abundance of 5 species including *Prevotella copri* ($\text{Log}_2(\text{MAM}/\text{well-nourished}) = 0.64$, MWU. $p=0.020$, MWU. $p=0.004$) and *Streptococcus sali-*

154 *varius* ($\text{Log2}(\text{MAM}/\text{Well-nourished}) = 2.39$, MWU $p=0.0005$, $q=0.032$)) in microbiomes from
 155 MAM infants, compared to well-nourished controls (Figure 1c). The increases in *P. copri* and *S.*
 156 *Salivarius*, were reciprocally associated with the depletion and reduction in the prevalence of the
 157 sphingolipid-producing species *Bacteroides fragilis* within the MAM microbiome ($\text{Log2}(\text{MAM}/\text{Well-}$
 158 $\text{nourished}=1.20$, MWU. $p=0.021$, $q=0.49$). This reciprocal relationship was observed as a trend in
 159 increase to the P/B ratio of the MAM infants ($\text{Log2}(\text{MAM}/\text{Well-nourished})=2.81$, MWU= 0.064)
 160 (Figure 1d). Functional pathway analyses revealed no significant differences in the composition
 161 of the overall functionome between MAM and well-nourished controls (PERMANOVA, $R^2=8.76$,
 162 $p=0.365$). After false discovery rate adjustment there were no significant differences in the path-
 163 way relative abundances (supp table). However, 19/525 pathways were differentially abundant
 164 using MWU without FDR adjustment between the conditions (Figure 1e, Supplementary Table
 165 X). Specifically, MAM gut microbiomes had an over-representation of pathways involved in branch
 166 chain amino acid biosynthesis ($\text{Log2}(\text{well-nourished}/\text{MAM})=-0.13$, MWU. $p=0.004$) including L-
 167 valine and L-isoleucine (I, III), fatty acid synthesis (PWY-7117 ($\text{Log2}(\text{well-nourished}/\text{MAM})=-$
 168 0.13 , MWU $p=0.004$) including, PWY0-862, PWY-7664, and PWY-6282), and sucrose/glucose
 169 degradation (PWY-5384 ($\text{Log2}(\text{well-nourished}/\text{MAM})=-0.19$, MWU $p=0.009$)). Conversely, there
 170 was a decrease in relative abundance anaerobic pathways including isopropanol biosynthesis ($\text{Log2}(\text{well-}$
 171 $\text{nourished}/\text{MAM})=1.03$, MWU $p=0.020$) and pyruvate fermentation pathways to the Short Chain
 172 Fatty Acid (SCFA) propionate ($\text{Log2}(\text{well-nourished}/\text{MAM}) = 0.37$, MWU $p=0.017$) within the
 173 MAM infant's gut.

174 **Malnutrition impacts brain activity and expressive communication**

175 Malnourished children often present with long-term impairments in neural and cognitive develop-
 176 ment. Resting state electroencephalography (EEG) assessments of participants were performed
 177 to enable investigation of the impacts of malnutrition on brain activity (Supp Table X,Y). After
 178 exploratory comparisons between EEG PSD between infants with MAM and our well-nourished
 179 controls, we will subsequently focus on the high-alpha (9-12 Hz), beta (12-30 Hz) and gamma
 180 (30-45 Hz) frequency bands distributed across occipital, temporal and frontal regions of interest.
 181 These bands are generally associated with concentration, alertness, and higher mental activity and
 182 were observed to have higher amplitudes in the well-nourished infants compared to infants with
 183 MAM (supp table).

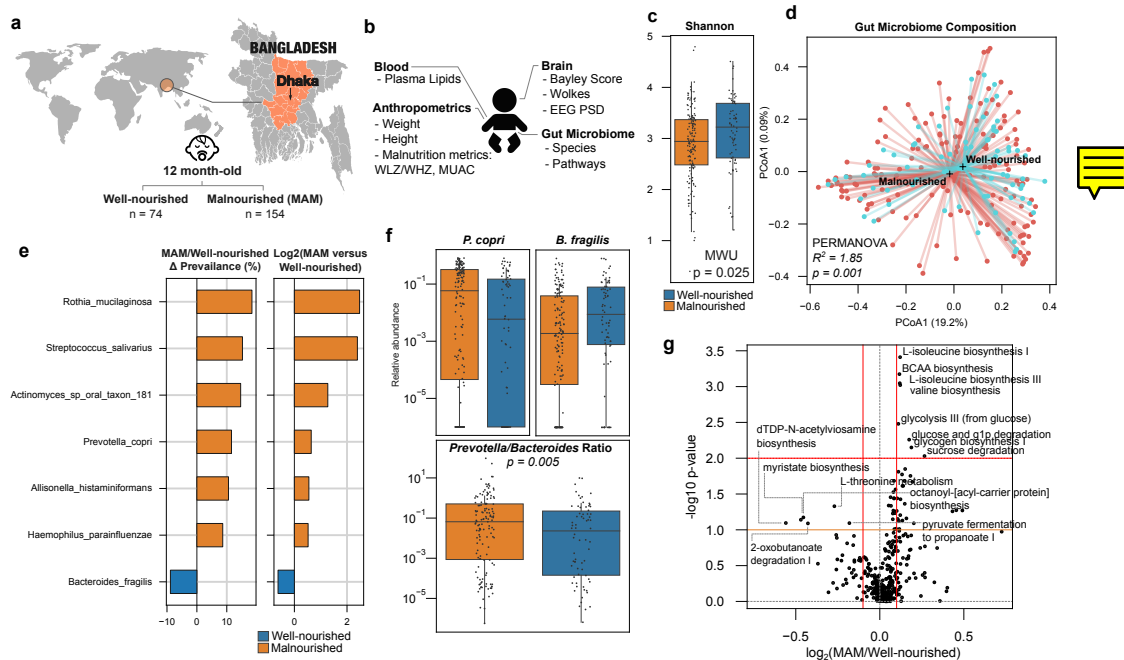


Figure 1: Malnutrition impacts the 12-month-old infant gut microbiome. a) Schematic of study design. b) Summary of data collected. c) Change in diversity of the gut microbiome associated with malnutrition. d) PCoA Scatterplot of Bray-Curtis beta diversities of samples (each marker is a single sample). e) Barplot of significant taxonomic differences in relative abundance and prevalence between 12-month-old well-nourished and MAM samples (MWU $p < 0.05$). f) Boxplot of P/B ratio change between study conditions. g) Volcano plot of pathways affected by malnutrition (upper left and upper right quadrants signify significant changes where the red horizontal line signifies MWU $q < 0.05$ and vertical lines represent \log_2 fold change of -0.1 and 0.1 respectively).

We used the Bayley Scales of Infant and Toddler Development Fourth Edition (BSID-IV; Bayley & Aylward, 2019) to assess development in our cohorts. When compared to well-nourished infants, there was a significant reduction in the Expressive Communication score in the MAM infants ($\log_2(\text{well-nourished}/\text{MAM})=0.10$, MWU. $p=0.02$). Expressive communication is a measure of how well a child communicates with others (Figure 2). However, there were no significant differences in receptive language, cognitive, or motor abilities.

Malnutrition is associated with a reduction in circulating lysolipids and ceramides

Adequate nutrition in infants is characterised by healthy circulating concentrations of metabolites, including lipids, involved in growth and development³³. Therefore, we used discovery LC-MS/MS

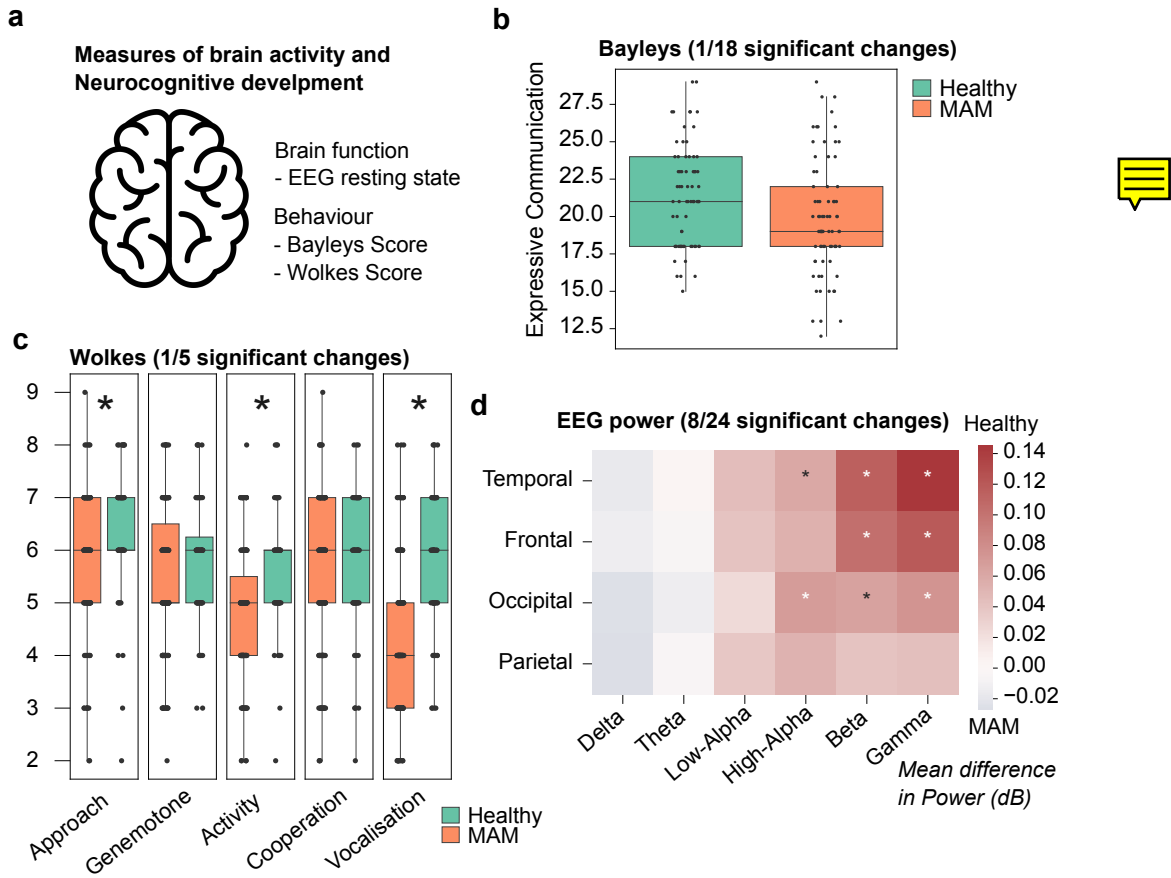


Figure 2: Differences in cognitive development of 12-month-old infants associate with malnutrition. a) Schematic of approach to study neurocognitive function. b) Boxplot of significant difference in Expressive Communication Score of the children with malnutrition compared to well-nourished controls. c) Heatmap of lobe and frequency specific changes in EEG resting state power spectral density (PSD) in MAM versus well-nourished infants. * = MWU $q < 0.05$.

194 to characterise and quantify the levels of 1041 lipids in plasma samples in our cohort of MAM and
195 well-nourished infants (Figure 3).

196 Malnutrition was associated with significant changes (309/1041 - 30%) to the plasma lipidome. Of
197 these changes, 140 (13%) plasma lipidome compounds increased and 169 (16%) decreased in con-
198 centration (Figure 3, supp table). We identified a reduction in the abundance of three lipid classes
199 with diverse functions, including two that are known to be specific to neurological development
200 and function (i.e. the long chain ceramide Cer 31:5;O2 ($\text{Log2}(\text{well-nourished}/\text{MAM})=2.44$, MWU
201 $q=2.51\text{e-}8$) and the lactosylceramide hex2cer 34:1 ($\text{Log2}(\text{well-nourished}/\text{MAM})=1.50$, MWU $q=0.004$)).
202 By contrast, long chain sphingomyelins (SM 44:3;O2, $\text{Log2}(\text{well-nourished}/\text{MAM})=-1.47$, MWU

203 $q=5.81e-5$) and others were observed to increase in relative concentration in malnourished infants.
 204 Several lysophospholipids from the Lysophosphatidylcholine (LPC), and Lysophosphatidylethanolamine
 205 (LPE) classes were enriched in well-nourished infant plasma.

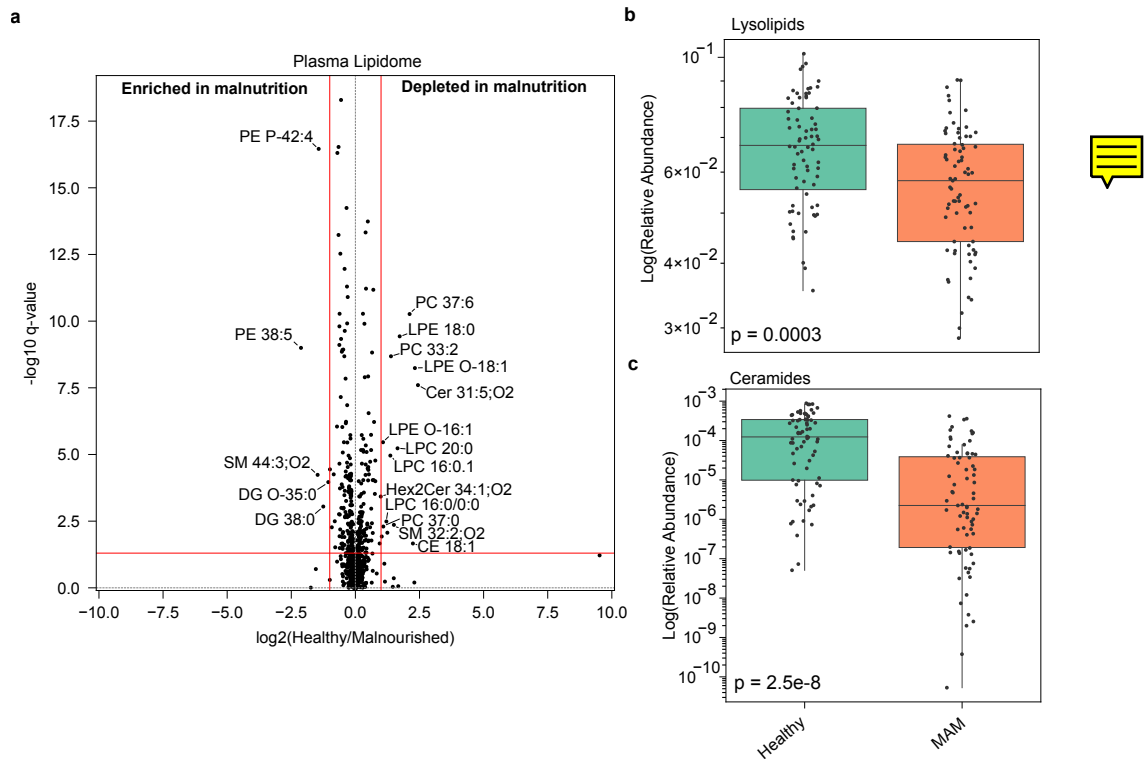


Figure 3: Malnutrition results in major, compositional differences in plasma lipids in 12-month-olds. Volcano plot changes to plasma lipids between well-nourished and MAM 1-year-olds. (Upper left and upper right quadrants signify significant changes where the red horizontal line signifies MWU $q < 0.05$ and vertical lines represent \log_2 fold change of -0.1 and 0.1 respectively). b) Lipidome class analysis. c) Ceramide abundance differences.

206 **Multimodal Random Forest classifiers** for malnutrition reveal cross mode
 207 **influences**

208 Having established the existence of changes associated with malnutrition across the gut micro-
 209 biome, brain, and plasma lipids, the relative importance of changes in each of these domains for

the prediction of malnutrition was measured. Individual and multimodal Random Forest classifiers were trained, using gut microbiome taxonomic and functional neuroimaging (EEG), lipidome and behavioural data (Bayley scale scores), to predict malnutrition in 12-month-old infants.

Within the predictors trained on individual feature sets, plasma lipids (AUCROC=1.00, oob=1.00) were the best predictor of malnutrition in 1-year-old infants, followed by brain/behavioural metrics (i.e., EEG, and Bayley AUCROC=0.83, oob=0.64), and the gut microbiome taxonomic and functional profiles (AUCROC=0.59, oob=0.59).

Ensemble models were trained on the combined dataset (i.e. gut microbiome taxonomic, gut microbiome functional, neuroimaging (EEG), lipidome and Bayley scale scores; METHODS) using 10-fold cross validation. SHAP scoring interpretation was performed to understand the workings of these models and importance of the features without the assumption of linearity of relationship between features (Figure 4). Those features that changed significantly were more likely to have high importance for the model prediction, (supp table). Comparison with the individual models indicated that inclusion of the other datasets into the ensemble models lead to the identification of non-linear features that contributed to the predictive power of the microbial species within the classification model. For example, these included MAM depleted *Faecalibacterium prausnitzii* (SHAP(well-nourished/MAM)=-0.0076), and *Odoribacter splanchnicus* (SHAP(well-nourished/MAM)=-0.0063) or MAM enriched *Bifidobacterium breve* (SHAP(well-nourished/MAM)=0.0074), and *Haemophilus parainfluenzae* (SHAP(well-nourished/MAM)=0.0065).

Network Analysis reveals the importance of *Bacteroides fragilis* in infant neurocognitive development

Network analysis is a useful tool to understand complex systems that emerge from interactions between multiple components. To better understand the complexities of feature changes and correlations between the EEG, behavior, microbial species and functions, and plasma metabolites, we mapped out their architecture using co-abundant network analysis. Spearman correlation of the features that were altered by malnutrition was calculated, filtered by significance ($q < 0.05$) (1052/3906 correlations, supp table). Finally, only edges with a spearman rho cut-off of > 0.2 were used to construct the network.

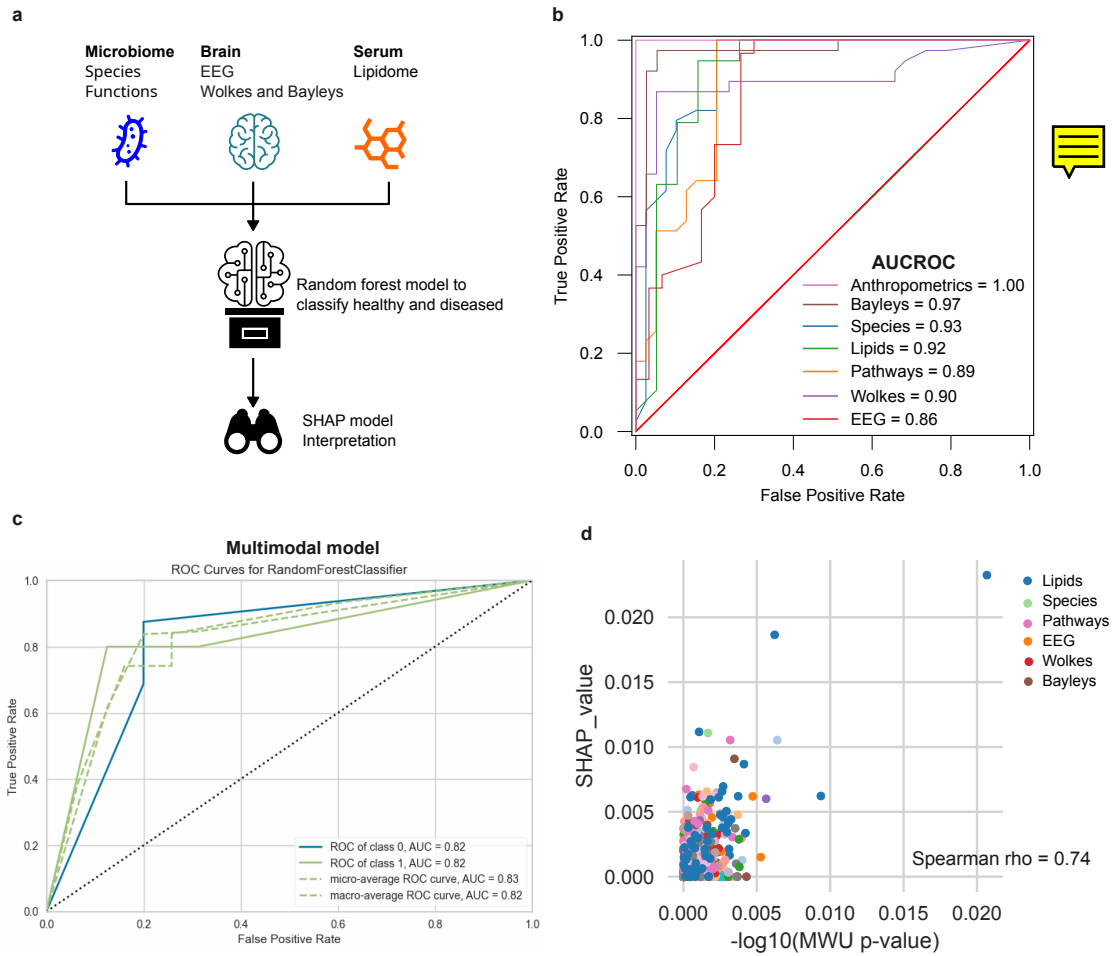


Figure 4: Integration of multimodal datasets boosts the predictive power and affects the relative feature importance of random forest models predicting nutritional status. a) Schematic describing interpreted multimodal approach to predict malnutrition. b) AUCROC curves showing relative predictive power of each modal dataset on predicting nutritional status. c) Multimodal model predicts malnutrition accurately. d) The multimodal model captures non-linear interactions between the features as demonstrated by the SHAP score distribution.

Important features (ie. mean absolute SHAP score > 0.002) were more likely to be significantly correlated ($q < 0.05$) with one another and had greater measures of Betweenness Centrality (Figure 5, Supplementary Table X) than unimportant features (mean absolute SHapley Additive exPlanations (SHAP) < 0.002). Plasma lipids that were enriched/depleted in the MAM condition (Supplementary Table X) were positively correlated with the anthropometric measures WLZ/WHZ, MUAC, and weight. Unsurprisingly, cluster analyses revealed that those features which were different between MAM and well-nourished were positively correlated with each other (i.e., change in the same direction, supp table). We identified a subcluster of *Bacteroides fragilis*,

pyruvate fermentation pathways, plasma ceramides, EEG PSD and Expressive Communication that was highly correlated with the well-nourished state (Figure 5, [supp table](#)). Those plasma lipids that were depleted (MWU. $q \leq 0.05$, $\text{Log}_2(\text{MAM}/\text{well-nourished}) \geq 0$) from the MAM infant samples were also positively correlated with EEG PSD amplitudes. Notably, EEG metrics were also correlated with bacterial pyruvate fermentation pathways that correlated with *B. fragilis* relative abundance. Conversely, we identified a highly correlated subcluster of *P. copri*, glycolysis, peptidoglycan biosynthesis, and BCAA pathways, and plasma sphingomyelins that are associated with the MAM condition.

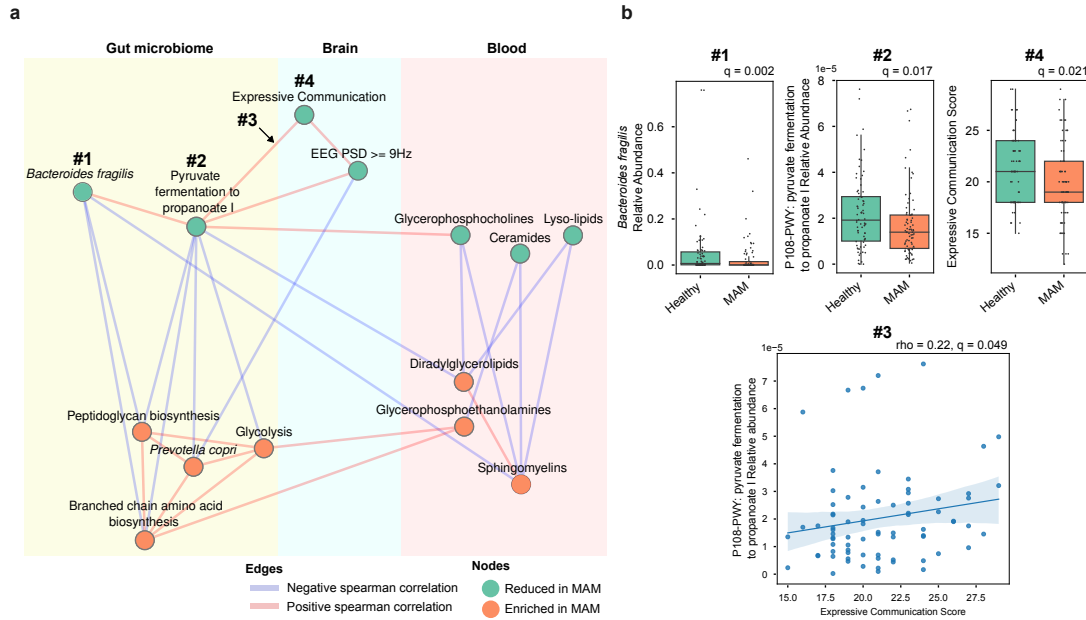


Figure 5: *Bacteroides fragilis* forms a network with propanoate synthesis, EEG and expressive communication that is anti-correlated with a *Prevotella copri* focused cluster of features in healthy and malnourished individuals. a) Network illustrating inter-relationships of feature associations that predict malnutrition. Inclusion in the network requires both a SHAP score for the node (> 0.6) and a significant Spearman rho score for the correlation of $q < 0.05$. Nodes are features coloured by their enrichment in MAM (orange and green are enriched and depleted in MAM respectively). Edges are spearman correlations coloured red and blue being positively and negatively correlated respectively. b) Evidence for relative abundance of *B. fragilis* (#1), pyruvate fermentation to propanoate I pathway relative abundance (#2), correlation between pyruvate fermentation to propanoate I pathway and Expressive communication (#3), Expressive communication score distributions (#4).

Discussion

A central goal of this study was to obtain a better understanding of how disturbances in host-microbiome interactions impact neurocognitive development in malnutrition. We observed that at the time of the malnutrition diagnosis and before administration of therapeutic feeds, malnutrition was characterised by a higher P/B ratio and lower anaerobic pathways such as pyruvate fermentation potential in the gut. *Prevotella* rich microbiomes have been typically understudied due to their underrepresentation in non LMIC³⁴. This ratio has previously been implicated in diet and lifestyle in adults³⁵ and *Bacteroides* have been observed previously to be depleted in Bangladesh infants¹⁸. Other studies of malnutrition have shown a decrease in alpha diversity which was unobserved in our population¹⁸. Accelerated ageing of the gut microbiome, as indicated by the presence of specific markers such as *P. copri* and *Bifidobacterium adolescentis*, is one possible hypothesis for the differential *Prevotella* abundance. Alternatively, selective microbiome community driven interactions might explain the inverse correlations that were observed between *P. copri* and *Bifidobacterium longum* and *B. breve*. *B. longum* and other anaerobic species have been previously linked to moderate and severe acute malnutrition in Bangladesh^{36;37}.

Comparisons of the MAM and control infants identified deficits both in neural activity and expressive communication that were associated with the malnourished condition. When investigating differences in neural activity, disruptions were evident for higher frequency power bands (alpha, beta, and gamma) but not lower frequency bands (delta and theta) in frontal, temporal and occipital areas. Therefore, we conclude that changes in expressive language are early and readily assessed indicators of long-term developmental consequences associated with MAM.

The plasma lipidomes of malnourished children were substantially different from those of controls, with significant differences in the levels of ceramides and lysolipids (i.e. lipid derivatives in which one or both acyl derivatives have been removed by hydrolysis). Numerous specific changes stand out as being potentially important for neural development. Firstly, lactosylceramide (hex2cer 34:1) is an essential precursor for synthesis of all complex glycosphingolipids³⁸ that was depleted by 50% in malnourished infants. Secondly, lysophosphatidylcholine (LPC) and lysophosphatidylethanolamine (LPE) are essential for brain development and growth as they carry fatty acid across the blood-brain barrier, via the major facilitator superfamily domain-containing protein 2A (Mfsd2a)³⁹.

284 Phosphatidylcholine (PC) is a precursor to acetylcholine, an essential neurotransmitter for memory
285 and cognitive function. Preliminary research suggests that higher levels of plasma PC35:6 may
286 be associated with better cognitive function in older adults and individuals with Alzheimer's
287 disease⁴⁰. Supplementing neuron differentiation medium with phosphatidylcholine reduces the
288 impact of inflammatory stress and neuronal damage, increasing the numbers of healthy neurons
289 and modulating neuronal plasticity⁴¹.

290 Propanoate has been demonstrated to be neuroprotective and induce neuroregeneration in the
291 peripheral nervous system during inflammation induced neuropathy. Conversely, higher serum
292 levels of propionic acid have been associated with increased odds of cognitive decline in a cohort
293 of > 65 year French individuals^{42;43}. Propanoate is a key precursor in lipid biosynthesis and
294 can be metabolised to propionyl-CoA, which can subsequently be incorporated into sphingolipid
295 biosynthesis pathways⁴⁴. It remains possible that this is due to extensive metabolic and microbial
296 programming during this period⁴⁵.

297 Random Forest classification models trained on the gut microbiome, neuroimaging data, and the
298 plasma lipidome accurately predicted the malnutrition condition. Combining SHAP values with
299 feature co-occurrence analysis revealed the importance of *Bacteroides fragilis* as a keystone species
300 for infant neurocognitive development. As there are less SMS, more of the ceramides are converted
301 to hexaceramides. Sphingomyelinases (SMases) hydrolyse sphingomyelin, releasing ceramide and
302 creating a cascade of bioactive lipids. These ceramides have been shown previously to be important
303 for myelin sheath development and so a depletion in this area may impact brain maturation.

304 Recent studies have emphasised the significant role of the gut microbiome in mediating dietary
305 effects on host physiology, in addition to its influence on the development and function of the
306 nervous system^{46;47;48;49}. Our cross-cohort analysis examined associations between infant mal-
307 nutrition, altered brain function, and the infant microbiome. However, in the absence of causal
308 animal studies, it remains unclear if the gut microbiome changes are a result of, or contribute
309 causally to the wider malnutrition phenotype.

310 Conclusion

311 Collectively, integrative multi-omic study highlights associations between the gut microbiome,
312 plasma lipids, brain connectivity, and cognitive function. The evidence we provide, may inform
313 the development of meaningful, targeted and effective interventions for infants experiencing mal-
314 nutrition.

315 Methods

316 Ethics

317 The M4EFaD intervention was registered [NCT05629624](#) on clinicaltrials.gov. The study was
318 approved by icddr,b Ethical Review Committee PR-21084 and the Bangladesh Directorate General
319 of Drug Administration. Ethical review for the analytical component was obtained from Auckland
320 Health Research Ethics Committee approval AH23922 (metabolomics, metagenomics, machine
321 learning).

322 Study Design and Participants

323 The study was performed on the baseline data from three cohorts of infants who were enrolled
324 (between Jan – December 2022) as part of the M4EFaD intervention within the Mirpur slum,
325 Dhaka, Bangladesh. The cohort consisted of: a control group of 73 well-nourished children at 12
326 ± 1 months (WLZ z-score > -1 SD); an intervention group of 156 children with WLZ < -2 and $>$
327 -3 z-score, and/or MUAC < 12.5 and > 11.5 cm having MAM at 12 ± 1 months; and an outcome
328 reference group of 73 children with WHZ < -2 and > -3 z-score, and/or MUAC < 12.5 and > 11.5
329 cm having stable MAM at 3 years ± 2 m. Inclusion criteria included a diagnosis of malnutrition,
330 no history of chronic medical conditions, and no antibiotic use within the past month. The study
331 protocol has been submitted for publication and is available on MedRxiv.

332 Recruitment and anthropometric data collection

333 Enrolment was initiated on February 7, 2022, and will continue until February 2024. Study
334 surveillance workers (SWs) conducted a door-to-door census (approximately 100,000 households)
335 in Mirpur DNCC wards ward 2, 3 and 5 between January and December 2022. Verbal consent
336 was obtained to participate in the census. The census identified 5736 children aged between 11 to
337 13 months and 2,314 children aged between 34 to 38 months. During the census, if the guardian
338 verbally consented to the study procedure, and the babies met the inclusion and exclusion criteria
339 of the study (Table 1), the SWs proceeded to measure the MUAC of the child. Mothers of
340 babies who were within the MUAC range were invited to visit the icddr,b study clinic for further
341 assessment and enrolment.

342 Final screening for eligibility and study consent occurred at the icddr,b Mirpur study clinic. The
343 consenting process was tailored to each mother’s literacy level and involved reviewing the inclusion
344 and exclusion criteria. Comprehension of the study was assessed using scripted points and open-
345 ended questions.

346 Following consent, the clinical screening team completed a screening form, capturing the date of
347 enrolment, sex, date of birth (DOB), weight (in kg), length/ height (in cm), head circumference
348 (in cm), and Mid-Upper Arm Circumference MUAC measurements of the child. The WLZ/WHZ
349 Z-score for each child was calculated using the WHO anthropometric calculator. The child’s age
350 was validated using the EPI vaccination card. Neurological measures, Bailey scores, EEG data
351 were collected upon enrolment to evaluate neurological development.

352 EEG data collection and analysis

353 Continuous scalp EEG was recorded using NetStation 4.5.4. and 128-channel Hydrocel Geodesic
354 Sensor Nets modified to remove eye electrodes (Electrical Geodesics, Inc. (EGI), Eugene, OR,
355 USA). Data was sampled at 500 Hz. Impedances were kept under 100 k Ω when possible and
356 measured once at the beginning of the session, and again halfway through. Sessions were conducted
357 in a dimly lit room with the participants sitting on the parent’s lap. The participants were
358 separated from the research staff conducting the session by a curtain, but the testing area was not
359 acoustically or electrically shielded. A second research staff member was present in the testing area

to help keep the participant engaged. EEG sessions consisted of 6 paradigms, i.e., resting state, visual working memory, flanker, disengagement, visual evoked potential, and auditory stimuli. The subsequent (pre-)processing steps were applied to the resting state data where participants watched a 3-minute video that featured toys.

EEG data were preprocessed offline with MatLab (R2021B) using the Harvard Automated Processing Pipeline for Electroencephalography (HAPPE) Version 3 (Gabard-Durnam et al., 2018). A specified subset of 30 channels was excluded ('E1', 'E8', 'E14', 'E17', 'E21', 'E25', 'E32', 'E38', 'E43', 'E44', 'E48', 'E49', 'E56', 'E63', 'E68', 'E73', 'E81', 'E88', 'E94', 'E99', 'E107', 'E113', 'E114', 'E119', 'E120', 'E121', 'E125', 'E126', 'E127', 'E128'). Data were downsampled to 250Hz, bandpass filtered (1-100Hz), and filtered using a 50Hz cleanline filter for line noise removal. Bad channels were then automatically identified and rejected, and wavelet-enhanced Independent Component Analysis (ICA) and the Multiple Artifact Rejection Algorithm (MARA) were performed to detect and impute artifacts. Resting state data were segmented into 2s epochs; epochs with an amplitude $\geq \pm 150\text{mV}$ were rejected. Segments were also rejected using segment similarity criteria. Data were then re-referenced to the average of all channels.

EEG outputs from HAPPE were then reformatted and processed using the Batch Electroencephalography Automated Processing Platform (BEAPP) (Levin et al., 2018) to extract power spectra for each participant across the following frequency bands: delta (2-4Hz), theta (4-6Hz), low alpha (6-9Hz), high alpha (9-12Hz), beta (12-30Hz), and gamma (30-45Hz) and the following regions of interest (see Supp Figure 2): occipital ('E70', 'E71', 'E75', 'E76', 'E83'), temporal ('E36', 'E40', 'E41', 'E45', 'E46', 'E102', 'E103', 'E104', 'E108', 'E109'), parietal ('E52', 'E53', 'E59', 'E60', 'E85', 'E86', 'E91', 'E92'), and frontal ('E5', 'E6', 'E12', 'E13', 'E24', 'E27', 'E28', 'E33', 'E34', 'E112', 'E116', 'E117', 'E122', 'E123', 'E124'). Further, PSD values were normalized by a log10 transform.

Developmental Outcomes (Bayley)

The Bayley Scales of Infant and Toddler Development, Fourth Edition (BSID-IV) cognitive, language, and motor subscales were administered to all participants. Research assistants were trained to research reliability in the administration and scoring of the Bayley-4. Due to cultural differences between the Bangladesh and the United States where the assessment was developed, Bangladeshi

researchers modified some assessment stimuli to improve cultural responsiveness and relevancy. For example, pictures for the item naming series and action naming series of the expressive language and receptive language subscales were adapted to include items that Bangladeshi children are more likely to be familiar with and bedtime clothing that would signify the child in the picture was going to sleep instead of the one-piece pajamas worn in the original picture, which the Bangladeshi children would not be familiar with.

Biological sample collection

Stool samples were collected from each infant at their home at the baseline visit. Samples were collected in DNA/RNA Shield Fecal Collection Tubes (Zymo Research, #R1101) and stored at (RT? -20? -80C?). Peripheral venous blood samples were collected in EDTA Vacutainers, separated into plasma and RBCs and immediately frozen at -80 C. Batches of blood and stool samples were air-freighted on dry ice from Bangladesh to the Liggins Institute, New Zealand for processing and analysis.

Microbiome DNA extraction and sequencing

DNA was extracted from stool samples using the ZymoBIOMICS MagBead DNA/RNA extraction kit (Zymo Research, #R2136) following the standard protocol. Samples (1mL) were mechanically lysed in bead bashing tubes using the MiniG tissue homogenizer prior to extraction of DNA. 200 µL of the sample was used post-bead bashing for extraction of DNA following the protocol. A volume of 50 µL of elute was collected in DNase/RNase Free Water. Samples with a DNA concentration < 14.5ng/µL were re-extracted following the ZymoBIOMICS DNA extraction protocol. Samples were sequenced (Illumina NovaSeq 150PE reads) to an average sequencing depth of 20M read-pairs/sample. Raw sequences were processed using BioBakery3 tools⁵⁰, specifically read quality filtering and human decontamination with KneadData (Version 1), taxonomic profiling with MetaPhlAn3 (Version 3.1, using the mpa.v31.CHOCOPhAn_201901 database) and functional profiling using presence/absence and abundance of microbial pathways with HUMAnN3 (Version 3.6). A minimum threshold of > 0.1% relative abundance and > 5% prevalence for all detected species was applied.

416 Plasma lipidomics

417 Plasma samples for lipidomics were thawed on ice and extracted according to a method modified
418 from Liu et al. (2016) Liu et al.⁵¹. Briefly, 10 μ L volume was placed in an amber glass autosampler
419 vial and 300 μ L of a mixture of Type 1 water, butanol, methanol, chloroform and SPLASH
420 Lipidomix in a ratio of 4:15:15:20:1 was added. The mixture was vortexed and sonicated at
421 room temperature before the protein precipitate was removed by centrifugation and an aliquot
422 of supernatant transferred to an amber glass autosampler for negative ionisation LC-MS/MS.
423 A second aliquot of supernatant was diluted 5 times with 75% IPA for positive ionisation LC-
424 MS/MS. A 5 μ L volume of each sample was injected onto a Phenomenex Kinetex F5 column (100
425 mm \times 2.1 mm \times 2.6 μ m) and lipids were separated using a ternary gradient of Type 1 water,
426 methanol and isopropanol containing ammonium acetate. Lipids were quantified and identified
427 with a Q-Exactive mass spectrometer (Thermo Fisher Scientific, Germany) equipped with a heated
428 electrospray ionisation [HESI] source. Data was processed using MS-DIAL v4.92 92⁵². For full
429 methodological details see the supplementary information.

430 Statistical Analyses

431 Python version 3.9.2 was used to perform all analysis⁵³. Due to the unequal sample sizes and
432 non-normally distributed data; non-parametric statistical approaches were used for differential
433 abundance analysis. Relative abundances were adjusted by Centred Log Ratio to account for
434 the compositional nature of the dataset⁵⁴. Log adjusted fold change significance was measured
435 using (MWU) test using the 'mannwhitneyu' function from 'scipy.stats' and adjusted for multiple
436 testing using the 'fdr correction' function from statsmodels.stats.multitest. Principal Coordinates
437 Analysis (PCoA) ordinations (plotted using 'skbio.stats.ordination.pcoa' module) were used to
438 visualise the clustering of the Bray-Curtis dissimilarities (calculated using skbio.distance.pdist)
439 between samples from their species and functional composition. To quantify the variance of the gut
440 microbiome explained covariates, PERMANOVA p-values were calculated from those Bray-Curtis
441 Dissimilarities using the 'permanova' function from the 'skbio.stats.distance' module. Bray-Curtis
442 were also used to capture the temporal dynamics of the microbiome from baseline. Numerical
443 Associations between species and metadata were measured with Spearman correlation (calculated
444 using 'spearmanr' function from 'scipy.stats' module), where significance was defined as False

445 Discovery Rate (FDR) adjusted p-values of < 0.05 ⁵⁵. Associations between categorical data were
446 measured with Fisher’s Exact test (calculated using ‘fisher_exact’ from ‘scipy.stats’ module), where
447 significance was defined as p-values of < 0.05 .

448 Machine learning

449 Machine learning models were used to classify malnourished from well-nourished infants. Extra-
450 trees Random Forest models were trained on functional and microbial taxa relative abundances.
451 Model hyperparameters including the number of trees in the forest, maximum tree depth, and
452 minimum sample numbers needed to split internal nodes were tuned using grid searching. A 5-
453 fold cross-validation was used to measure the performance of each hyperparameter combination
454 and to identify overfitting. Model performance was measured with AUCROC and out-of-bag error
455 analysis (oob). SHAP Value (SHapley Additive exPlanations) interpretation was used to interpret
456 the contributions each feature had on the model’s performance using the ‘shap’ python package
457 lundberg2017unified.

458 Network analysis

459 Absolute spearman rho of above 0.3 were used as edges and gut bacterial species and functional
460 profiles, EEG, and plasma lipids were used as nodes coloured by their mean directional SHAP
461 scores for classifier models that distinguish MAM from well-nourished conditions. Centrality and
462 edge-betweenness were calculated with the ‘networkx’ python package REF.

463 Code availability

464 All analysis code is available on the GitHub repository. The codebase is organised into scripts,
465 providing a comprehensive framework for replicating the experiments. Detailed documentation
466 and instructions on how to use the code are provided in the repository’s README file.

467 **Declarations**

468 **Ethics approval and consent to participate**

469 Ethical approvals were obtained from the Research Review Committee (RRC; August 21, 2021)
470 and Ethical Review Committee (ERC) of icddr,b (protocol no: PR-21084; September 21, 2021),
471 Institutional Review Board of Boston Children’s Hospital, USA (for analyses of neuropsychological
472 assessments), University of Auckland, New Zealand (approval AH23922; for analyses of collected
473 biological samples) and University of West Indies (CREC-MN.51, 21/22).

474 **Data availability**

475 Metagenome data is available at [PRJNAXXX](#) on the SRA. EEG and metadata are available from
476 the authors, upon reasonable request that meets the ethics of the study.

477 **Competing interests**

478 The authors declare that they have no competing interests.

479 **Funding**

480 Work on this clinical trial is supported by Wellcome Leap (9942 Culver Blvd Unit 1277 Culver
481 City, CA 90232-4167, United States; [WWW.WELLCOMELEAP.ORG](#)) to PDG, JMO, TF and
482 CAN as part of the 1kD Program. We acknowledge our core donors, Governments of Bangladesh,
483 Canada for providing unrestricted support and commitment to icddr,b’s research effort.

Author Contributions

TP, KG and JOS drafted and co-wrote the manuscript. TS, SHK, BCW, BH, CP, AB, DH, IS, AME, RD, GG, CK, PDG, RH, TF, CAN commented on the manuscript. JMO, RH, TF, PDG, CAN designed the study and analyses. TS, SHK performed assessments and obtained samples in Dhaka. RH oversaw the Dhaka group. TP performed multiomic analyses, BCW and IS performed metagenomics, CP performed metabolomics, JOS oversaw the Auckland group. BH performed EEG analyses, CAN oversaw the Boston group.

Acknowledgements

The authors would like to acknowledge the participants in Mirpur, Dhaka, Bangladesh for their contributions to this study. The authors would also like to thank the study team within the Infectious Diseases Division, International Centre for Diarrheal Disease Research, Bangladesh for their work in participant recruitment, sample collection and assessments.

References

- [1] Mercedes De Onis, Monika Blossner, World Health Organization, et al. Who global database on child growth and malnutrition. Technical report, World Health Organization, 1997.
- [2] Reynaldo Martorell and Teresa J Ho. Malnutrition, morbidity, and mortality. *Population and Development Review*, 10:49–68, 1984.
- [3] Anett Nyaradi, Jianghong Li, Siobhan Hickling, Jonathan Foster, and Wendy H Oddy. The role of nutrition in children’s neurocognitive development, from pregnancy through childhood. *Frontiers in human neuroscience*, 7:97, 2013.
- [4] Dean T Jamison. Child malnutrition and school performance in china. *Journal of development economics*, 20(2):299–309, 1986.
- [5] Jeremy E Koenig, Aymé Spor, Nicholas Scalfone, Ashwana D Fricker, Jesse Stombaugh, Rob Knight, Largus T Angenent, and Ruth E Ley. Succession of microbial consortia in the

508 developing infant gut microbiome. *Proceedings of the National Academy of Sciences*, 108
509 (supplement_1):4578–4585, 2011.

510 [6] Chiara Morreale, Cristina Giaroni, Andreina Baj, Laura Folgari, Lucia Barcellini, Amraj
511 Dhimi, Massimo Agosti, and Ilia Bresesti. Effects of perinatal antibiotic exposure and neonatal
512 gut microbiota. *Antibiotics*, 12(2):258, 2023.

513 [7] Hagay Enav, Fredrik Bäckhed, and Ruth E Ley. The developing infant gut microbiome: a
514 strain-level view. *Cell Host & Microbe*, 30(5):627–638, 2022.

515 [8] Ruairi C Robertson, Thaddeus J Edens, Lynnea Carr, Kuda Mutasa, Ethan K Gough, Ceri
516 Evans, Hyun Min Geum, Iman Baharmand, Sandeep K Gill, Robert Ntozini, et al. The gut
517 microbiome and early-life growth in a population with high prevalence of stunting. *Nature
518 communications*, 14(1):654, 2023.

519 [9] Fanette Fontaine, Sondra Turjeman, Karel Callens, and Omry Koren. The intersection of
520 undernutrition, microbiome, and child development in the first years of life. *Nature Commu-
521 nications*, 14(1):1–9, 2023.

522 [10] Robert Y Chen, Ishita Mostafa, Matthew C Hibberd, Subhasish Das, Mustafa Mahfuz, Nu-
523 run N Naila, M Munirul Islam, Sayeeda Huq, M Ashraful Alam, Mahabub U Zaman, et al.
524 A microbiota-directed food intervention for undernourished children. *New England Journal
525 of Medicine*, 384(16):1517–1528, 2021.

526 [11] Laura V Blanton, Mark R Charbonneau, Tarek Salih, Michael J Barratt, Siddarth Venkatesh,
527 Olga Ilkaveya, Sathish Subramanian, Mark J Manary, Indi Trehan, Josh M Jorgensen, et al.
528 Gut bacteria that prevent growth impairments transmitted by microbiota from malnourished
529 children. *Science*, 351(6275):aad3311, 2016.

530 [12] Caroline Kelsey, Caitlin Dreisbach, Jeanne Alhusen, and Tobias Grossmann. A primer on
531 investigating the role of the microbiome in brain and cognitive development. *Developmental
532 Psychobiology*, 61(3):341–349, 2019.

533 [13] Caroline M Kelsey, Stephanie Prescott, John A McCulloch, Giorgio Trinchieri, Tara L Val-
534 ladares, Caitlin Dreisbach, Jeanne Alhusen, and Tobias Grossmann. Gut microbiota compo-
535 sition is associated with newborn functional brain connectivity and behavioral temperament.
536 *Brain, Behavior, and Immunity*, 91:472–486, 2021.

- [14] Inmaculada Acuña, Tomás Cerdó, Alicia Ruiz, Francisco J Torres-Espínola, Ana López-Moreno, Margarita Aguilera, Antonio Suárez, and Cristina Campoy. Infant gut microbiota associated with fine motor skills. *Nutrients*, 13(5):1673, 2021.
- [15] Alexander L Carlson, Kai Xia, M Andrea Azcarate-Peril, Barbara D Goldman, Mihye Ahn, Martin A Styner, Amanda L Thompson, Xiujuan Geng, John H Gilmore, and Rebecca C Knickmeyer. Infant gut microbiome associated with cognitive development. *Biological psychiatry*, 83(2):148–159, 2018.
- [16] Bhoomika R Kar, Shobini L Rao, and BA Chandramouli. Cognitive development in children with chronic protein energy malnutrition. *Behavioral and Brain Functions*, 4(1):1–12, 2008.
- [17] Remco Kort, Job Schlösser, Alan R Vazquez, Prudence Atukunda, Grace KM Muhoozi, Alex Paul Wacoo, Wilbert FH Sybesma, Ane C Westerberg, Per Ole Iversen, and Eric D Schoen. Model selection reveals the butyrate-producing gut bacterium coprococcus eutactus as predictor for language development in 3-year-old rural ugandan children. *Frontiers in microbiology*, 12:681485, 2021.
- [18] Kassandra Roger, Phetsamone Vannasing, Julie Tremblay, Maria L Bringas Vega, Cyralene P Bryce, Arielle G Rabinowitz, Pedro A Valdés-Sosa, Janina R Galler, and Anne Gallagher. Impact of early childhood malnutrition on adult brain function: An evoked-related potentials study. *Frontiers in Human Neuroscience*, 16:884251, 2022.
- [19] PM Udani. Protein energy malnutrition (pem), brain and various facets of child development. *The Indian Journal of Pediatrics*, 59:165–186, 1992.
- [20] Wei Gao, Andrew P Salzwedel, Alexander L Carlson, Kai Xia, M Andrea Azcarate-Peril, Martin A Styner, Amanda L Thompson, Xiujuan Geng, Barbara D Goldman, John H Gilmore, et al. Gut microbiome and brain functional connectivity in infants-a preliminary study focusing on the amygdala. *Psychopharmacology*, 236:1641–1651, 2019.
- [21] Kadi Vaher, Debby Bogaert, Hilary Richardson, and James P Boardman. Microbiome-gut-brain axis in brain development, cognition and behavior during infancy and early childhood. *Developmental Review*, 66:101038, 2022.
- [22] Anne V Kane, Duy M Dinh, and Honorine D Ward. Childhood malnutrition and the intestinal microbiome. *Pediatric research*, 77(1):256–262, 2015.

- [23] Manu S Goyal, Siddarth Venkatesh, Jeffrey Milbrandt, Jeffrey I Gordon, and Marcus E Raichle. Feeding the brain and nurturing the mind: linking nutrition and the gut microbiota to brain development. *Proceedings of the National Academy of Sciences*, 112(46):14105–14112, 2015.
- [24] Prudence Atukunda, Grace KM Muhoozi, Tim J Van Den Broek, Remco Kort, Lien M Diep, Archileo N Kaaya, Per O Iversen, and Ane C Westerberg. Child development, growth and microbiota: follow-up of a randomized education trial in uganda. *Journal of global health*, 9(1), 2019.
- [25] Per Ole Iversen, Prudence Atukunda, Remco Kort, Per Magne Ueland, Ane Cecilie West-erberg, and Grace Kyamazima Mehangye Muhoozi. No associations between microbiota signaling substances and cognitive, language and motor development among three-year-old rural ugandan children. *Acta Paediatrica*, 2020.
- [26] Sidhartha Das, Bibhuti B Tripathy, Kshitish C Samal, and Nimai C Panda. Plasma lipids and lipoprotein cholesterol in undernourished diabetic subjects and adults with protein energy malnutrition. *Diabetes Care*, 7(6):579–586, 1984.
- [27] Gabriela RS Veiga, Haroldo S Ferreira, Ana L Sawaya, Jairo Calado, and Telma MMT Florêncio. Dyslipidaemia and undernutrition in children from impoverished areas of maceió, state of alagoas, brazil. *International journal of environmental research and public health*, 7(12):4139–4151, 2010.
- [28] Th Hornemann. Mini review: lipids in peripheral nerve disorders. *Neuroscience letters*, 740:135455, 2021.
- [29] Cristhyane Costa De Aquino, Ricardo A Leitão, Luís A Oliveira Alves, Vanessa Coelho-Santos, Richard L Guerrant, Carlos F Ribeiro, João O Malva, Ana P Silva, and Reinaldo B Oriá. Effect of hypoproteic and high-fat diets on hippocampal blood-brain barrier permeability and oxidative stress. *Frontiers in nutrition*, 5:131, 2019.
- [30] Santosh Lamichhane, Partho Sen, Marina Amaral Alves, Henrique C Ribeiro, Peppi Raunioniemi, Tuulia Hyötyläinen, and Matej Orešič. Linking gut microbiome and lipid metabolism: moving beyond associations. *Metabolites*, 11(1):55, 2021.
- [31] Tahmeed Ahmed, Mustafa Mahfuz, Santhia Ireen, AM Shamsir Ahmed, Sabuktagin Rahman, M Munirul Islam, Nurul Alam, M Iqbal Hossain, SM Mustafizur Rahman, M Mohsin Ali, et al.

- 596 Nutrition of children and women in bangladesh: trends and directions for the future. *Journal*
597 *of health, population, and nutrition*, 30(1):1, 2012.
- 598 [32] Lindsey Lenters, Kerri Wazny, and Zulfiqar A Bhutta. Management of severe and moderate
599 acute malnutrition in children. *Reproductive, maternal, newborn, and child health: disease*
600 *control priorities. 3rd edition. Washington, DC: World Bank*, pages 205–223, 2016.
- 601 [33] Asha V Badaloo, Terrence Forrester, Marvin Reid, and Farook Jahoor. Lipid kinetic differ-
602 ences between children with kwashiorkor and those with marasmus. *The American journal*
603 *of clinical nutrition*, 83(6):1283–1288, 2006.
- 604 [34] Adrian Tett, Kun D Huang, Francesco Asnicar, Hannah Fehlner-Peach, Edoardo Pasolli,
605 Nicolai Karcher, Federica Armanini, Paolo Manghi, Kevin Bonham, Moreno Zolfo, et al.
606 The prevotella copri complex comprises four distinct clades underrepresented in westernized
607 populations. *Cell host & microbe*, 26(5):666–679, 2019.
- 608 [35] Mads F Hjorth, Trine Blædel, Line Q Bendtsen, Janne K Lorenzen, Jacob B Holm, Pia Ki-
609 ilerich, Henrik M Roager, Karsten Kristiansen, Lesli H Larsen, and Arne Astrup. Prevotella-
610 to-bacteroides ratio predicts body weight and fat loss success on 24-week diets varying in
611 macronutrient composition and dietary fiber: results from a post-hoc analysis. *International*
612 *Journal of Obesity*, 43(1):149–157, 2019.
- 613 [36] Michael J Barratt, Sharika Nuzhat, Kazi Ahsan, Steven A Frese, Aleksandr A Arzamasov,
614 Shafiqul Alam Sarker, M Munirul Islam, Parag Palit, Md Ridwan Islam, Matthew C Hibberd,
615 et al. Bifidobacterium infantis treatment promotes weight gain in bangladeshi infants with
616 severe acute malnutrition. *Science Translational Medicine*, 14(640):eabk1107, 2022.
- 617 [37] Matthieu Million, Maryam Tidjani Alou, Saber Khelaifia, Dipankar Bachar, Jean-Christophe
618 Lagier, Niokhor Dione, Souleymane Brah, Perrine Hugon, Vincent Lombard, Fabrice Ar-
619 mougom, et al. Increased gut redox and depletion of anaerobic and methanogenic prokaryotes
620 in severe acute malnutrition. *Scientific reports*, 6(1):26051, 2016.
- 621 [38] Giovanni D’Angelo, Serena Capasso, Lucia Sticco, and Domenico Russo. Glycosphingolipids:
622 synthesis and functions. *The FEBS journal*, 280(24):6338–6353, 2013.
- 623 [39] Shu Ting Tan, Tejasvene Ramesh, Xiu Ru Toh, and Long N Nguyen. Emerging roles of
624 lysophospholipids in health and disease. *Progress in Lipid Research*, 80:101068, 2020.

- [40] Mei-Hua Qu, Xiaoyun Yang, Yuming Wang, Qingjuan Tang, Hailin Han, Jia Wang, Guo-Du Wang, Changhu Xue, and Zhiqin Gao. Docosaheptaenoic acid-phosphatidylcholine improves cognitive deficits in an $\alpha\beta 23$ -35-induced alzheimer’s disease rat model. *Current Topics in Medicinal Chemistry*, 16(5):558–564, 2016.
- [41] Dario Magaquian, Susana Delgado Ocaña, Consuelo Perez, and Claudia Banchio. Phosphatidylcholine restores neuronal plasticity of neural stem cells under inflammatory stress. *Scientific reports*, 11(1):22891, 2021.
- [42] Jeanne Neuffer, Raúl González-Domínguez, Sophie Lefèvre-Arbogast, Dorrain Y Low, Bénédicte Driollet, Catherine Helmer, Andrea Du Preez, Chiara de Lucia, Silvie R Ruigrok, Barbara Altendorfer, et al. Exploration of the gut–brain axis through metabolomics identifies serum propionic acid associated with higher cognitive decline in older persons. *Nutrients*, 14(21):4688, 2022.
- [43] Thomas Grüter, Nuwin Mohamad, Niklas Rilke, Alina Blusch, Melissa Sgodzai, Seray Demir, Xiomara Pedreiturria, Katharina Lemhoefer, Barbara Gisevius, Aiden Haghighi, et al. Propionate exerts neuroprotective and neuroregenerative effects in the peripheral nervous system. *Proceedings of the National Academy of Sciences*, 120(4):e2216941120, 2023.
- [44] Natsuki Kondo, Yusuke Ohno, Maki Yamagata, Takashi Obara, Naoya Seki, Takuya Kitamura, Tatsuro Naganuma, and Akio Kihara. Identification of the phytosphingosine metabolic pathway leading to odd-numbered fatty acids. *Nature communications*, 5(1):5338, 2014.
- [45] Iqbal Mahmud, Mamun Kabir, Rashidul Haque, and Timothy J Garrett. Decoding the metabolome and lipidome of child malnutrition by mass spectrometric techniques: present status and future perspectives. *Analytical chemistry*, 91(23):14784–14791, 2019.
- [46] Christina N Heiss and Louise E Olofsson. The role of the gut microbiota in development, function and disorders of the central nervous system and the enteric nervous system. *Journal of neuroendocrinology*, 31(5):e12684, 2019.
- [47] Florencia Ceppa, Andrea Mancini, and Kieran Tuohy. Current evidence linking diet to gut microbiota and brain development and function. *International journal of food sciences and nutrition*, 70(1):1–19, 2019.
- [48] Tatiana Milena Marques, John F Cryan, Fergus Shanahan, Gerald F Fitzgerald, R Paul Ross, Timothy G Dinan, and Catherine Stanton. Gut microbiota modulation and implications for

- 655 host health: Dietary strategies to influence the gut–brain axis. *Innovative Food Science &*
656 *Emerging Technologies*, 22:239–247, 2014.
- 657 [49] Thomas C Fung, Christine A Olson, and Elaine Y Hsiao. Interactions between the microbiota,
658 immune and nervous systems in health and disease. *Nature neuroscience*, 20(2):145–155, 2017.
- 659 [50] Francesco Beghini, Lauren J McIver, Aitor Blanco-Míguez, Leonard Dubois, Francesco As-
660 ninar, Sagun Maharjan, Ana Mailyan, Paolo Manghi, Matthias Scholz, Andrew Maltez
661 Thomas, et al. Integrating taxonomic, functional, and strain-level profiling of diverse mi-
662 crobial communities with biobakery 3. *elife*, 10:e65088, 2021.
- 663 [51] Xinyu Liu, Jia Li, Peng Zheng, Xinjie Zhao, Chanjuan Zhou, Chunxiu Hu, Xiaoli Hou,
664 Haiyang Wang, Peng Xie, and Guowang Xu. Plasma lipidomics reveals potential lipid markers
665 of major depressive disorder. *Analytical and bioanalytical chemistry*, 408:6497–6507, 2016.
- 666 [52] Hiroshi Tsugawa, Tomas Cajka, Tobias Kind, Yan Ma, Brendan Higgins, Kazutaka Ikeda,
667 Mitsuhiro Kanazawa, Jean VanderGheynst, Oliver Fiehn, and Masanori Arita. Ms-dial: data-
668 independent ms/ms deconvolution for comprehensive metabolome analysis. *Nature methods*,
669 12(6):523–526, 2015.
- 670 [53] Guido Van Rossum and Fred L Drake Jr. *Python reference manual*. Centrum voor Wiskunde
671 en Informatica Amsterdam, 1995.
- 672 [54] Gregory B Gloor, Jia Rong Wu, Vera Pawlowsky-Glahn, and Juan José Egozcue. It’s all
673 relative: analyzing microbiome data as compositions. *Annals of epidemiology*, 26(5):322–329,
674 2016.
- 675 [55] Pauli Virtanen, Ralf Gommers, Travis E. Oliphant, Matt Haberland, Tyler Reddy, David
676 Cournapeau, Evgeni Burovski, Pearu Peterson, Warren Weckesser, Jonathan Bright, Stéfan J.
677 van der Walt, Matthew Brett, Joshua Wilson, K. Jarrod Millman, Nikolay Mayorov, An-
678 drew R. J. Nelson, Eric Jones, Robert Kern, Eric Larson, C J Carey, İlhan Polat, Yu Feng,
679 Eric W. Moore, Jake VanderPlas, Denis Laxalde, Josef Perktold, Robert Cimrman, Ian Hen-
680 riksen, E. A. Quintero, Charles R. Harris, Anne M. Archibald, Antônio H. Ribeiro, Fabian
681 Pedregosa, Paul van Mulbregt, and SciPy 1.0 Contributors. SciPy 1.0: Fundamental Al-
682 gorithms for Scientific Computing in Python. *Nature Methods*, 17:261–272, 2020. doi:
683 10.1038/s41592-019-0686-2.

684 **Supplementary material**